Springer

Acta Mechanica Sinica

CrossMark click for updates

• RESEARCH PAPER •

Acta Mech. Sin., Vol. 39, 622461 (2023)
https://doi.org/10.1007/s10409-023-22461-x

Theoretical modeling of trail formation of a migrating neutrophil on substrate

Xiaoning Zhang[1,2], Wenhui Hu[1], Wenbo Gao[1], Yan Zhang[1,2*], and Mian Long[1,2*]

[1] *Center for Biomechanics and Bioengineering, Beijing Key Laboratory of Engineered Construction and Mechanobiology and Key Laboratory of Microgravity (National Microgravity Laboratory), Institute of Mechanics, Chinese Academy of Sciences, Beijing 100190, China;*
[2] *School of Engineering Sciences, University of Chinese Academy of Sciences, Beijing 100049, China*

Received January 4, 2023; accepted January 19, 2023; published online May 23, 2023

Neutrophils undergo fast migration dynamics onto endothelium or extracellular matrix using anterior protrusion together with posterior contraction and retraction. While these migrating cells tend to leave behind the long-lasting membranous trails with enriched integrins ripped down from cell body, it is still unclear how the trail formation is quantitatively correlated with cell migration and what the regulating factors are key in this process. Here a multi-layered mechanochemical model was integrated with a motor-clutch model to simulate numerically the chemotactic migration of a neutrophil on the substrate. Results indicated that, in response to those polarized distributions of sensing molecule P21-activated kinase 1 (PAK1) and the downstream molecules Ras-related C3 botulinum toxin substrate (Rac) and Ras homolog family member (RhoA), membrane-bound integrins tend to be accumulated at both the cell front and rear, promoting the increase of migrating velocity and trail number with time when actin-related protein2/3 complex (Arp2/3) and myosin are respectively accumulated at the front and rear. These predictions were in agreement with those typical experimental observations in integrin polarization and trail formation. Parametric analysis further proposed that, while the migrating velocity yields a biphasic dependence on substrate hardness and motor unloaded velocity, trail number increases monotonically with substrate hardness, on-rate of integrin-ligand bonds, motor unloaded velocity, motor stall force, and clutch number but decreases with chemokine concentration and off-rate of integrin-ligand bonds. This work provided an insight in elaborating the mechanochemical pathways in neutrophil migration and deciphering the key extracellular or intracellular factors in regulating the relevant trail formation of those migrating neutrophils.

Neutrophil migration, Trail formation, Theoretical modeling, Numerical calculation, Parametric analysis

Citation: X. Zhang, W. Hu, W. Gao, Y. Zhang, and M. Long, Theoretical modeling of trail formation of a migrating neutrophil on substrate, Acta Mech. Sin. **39**, 622461 (2023), https://doi.org/10.1007/s10409-023-22461-x

1. Introduction

Neutrophils are the first cell type that crosses the vascular endothelium into the tissues and reach the site of inflammation in inflammatory responses [1,2], serving as the key players that help organs initiate and maintain immune reactions and shape the overall immune response [3]. Neutrophil migration is affected by multiple physical and biochemical factors, reflecting its durotaxis or chemotaxis features. When exposed to an attractant gradient (i.e., fMet-Leu-Phe or fMLP), chemoattractants bind to transmembrane receptors that couple to heterotrimeric G proteins, leading to their dissociation into α- and βγ-subunits and then activating a plethora of effectors. These events in turn orchestrate a signaling cascade that ultimately gives rise to cellular polarization and movement. Indeed, dynamic features of neutrophil chemotaxis are a consequence of redistribution of intracellular signaling molecules. That is, Ras-related C3 botulinum toxin substrate (Rac), cell division control protein 42 homolog (Cdc42), and phosphatidylinositol (3,4,5)-trisphosphate (PIP3) that are associating with actin branching

*Corresponding authors. E-mail addresses: zhangyan@imech.ac.cn (Yan Zhang); mlong@imech.ac.cn (Mian Long)
Executive Editor: Yue Shao

and growth are enriched at the cell front or leading edge, while Ras homolog family member A (RhoA), phosphatidylinositol (4,5)-bisphosphate (PIP2), and phosphatase and tensin homolog (PTEN) that are correlating with myosin-II-induced contraction are assembled on the sides and at the rear or trailing edge [4]. The acquisition of polarity is accompanied by a dramatic redistribution of β_2 integrin and cytoskeletal components, during which neutrophils quickly orient themselves and move forward using anterior lamellipodia extension together with posterior contraction and retraction [5]. While existing evidences revealed that migrating neutrophils leave behind long-lasting, chemokine- and β_2 integrin-containing trails on intercellular adhesion molecule 1 (ICAM-1) coated substrate [6], it still remains unclear how these β_2 integrins are extracted from the cell membrane during neutrophil migration.

Neutrophil migration is coordinated by involving the formation and disassembly of cell adhesion sites, together with dynamic changes in actin cytoskeleton network [7,8]. Actin polymerization and integrin adhesion are spatio-temporally coordinated [9]. To achieve the migration, cells must exert forces on their substrate to propel the cell body forward. Inside the cells, force generation can be accomplished through actin-related protein2/3 complex (Arp2/3)-mediated F-actin self-assembly at the plasma membrane to push the membrane forward [10], or myosin motor-driven contractions that pull F-actin rearward to generate F-actin retrograde flow [11]. Intracellularly-generated forces are transmitted to the substrate by adhesion anchorages between the cell and the substrate, generating the traction forces that propel the cell forward [12-14]. In neutrophils, β_2 integrins act as intracellular clutches that transmit forces to the extracellular matrix (ECM) [15]. The extracellular domains of a β_2 integrin are bound to its ICAM-1 ligand on one side and its cytoplasmic domains are connected by focal adhesions (FAs) to actin bundle on the other side, coupling the retrograde actin flow to the underlying substrate [16-18]. Thus β_2 integrins act as an adjustable molecular clutch by mediating transient, indirect interactions between the retrograde-moving actin cytoskeleton and ICAM-1, so-called the "motor-clutch" model, and transfer external forces from ECM into the cell. While this mechanism proposes dynamic and differential engagement between the actin network and the substrate, in turn allowing a cell to sense and react to its environment [19], it is still unclear how this "motor-clutch" model works cooperatively with cytoskeletal polarization of a migrating neutrophil, especially for the trail formation.

Neutrophil movement on ICAM-1 is achieved through a well-described protrusion-adhesion-retraction cycle [20-24]: (1) Pushing forces at the cell front are generated by actin-polymerization and lead to protrusion of the lamellipodium; (2) Retrograde actin flow is connected to the substrate via focal adhesions, which leads to forward movement of the cell; and (3) Retraction of the cell posterior then occurs due to rear contraction and release of focal adhesions at the cell rear. During cell migration, neutrophil-substrate adhesions are highly dynamic, yielding continuous formation at the cell front and disruption at the cell rear to drive the cell movement [25]. Breakage of cell-substrate adhesions required for cell locomotion can occur either by intracellular disruption of cytoskeleton-β_2 integrin linkage (the upper site) or by extracellular release of β_2 integrin-ICAM-1 linkage (the lower site). For the former, the integrins can be extracted from cell body and the trails can be formed. Evidently, this process is quite complicated and regulated by various biomechanical and biochemical factors. Thus both chemotactic and mechanochemical modeling are theoretically important in understanding neutrophil migration dynamics [26]. On one hand, while one of the previous cell migration models is able to predict the chemotactic migration dynamics of an entire cell and the effects of substrate hardness on integrin-mediated traction [26], it only verifies the generation of circumferential forces but not the formation of trails [27]. On the other hand, the localized migration model for a part of the cell is able to depict the process of trail formation but hard to be extended for the entire cell [28,29]. Meanwhile, the motor-clutch model is beneficial to improve existing mechanochemical models in elucidating those mechanotransductive mechanisms in trail formation, since it reveals how cells interact with the substrate and what the parameters are crucial in regulating this durotaxis at the cellular level [30]. However, it is still lacking in elaborating the trail formation of a migrating cell from both chemotactic and mechanochemical aspects.

Here a multi-layered signaling mechanochemical model, proposed previously for cell chemotaxis, was integrated with a motor-clutch model for predicting theoretically the intracellular mechanotransduction. Based on the experimental observation of remnant trails left behind migrating neutrophils, numerical calculations were conducted to correlate cell migration behaviors with cell-substrate interactions and intracellular signaling pathways. Parametric analysis dissected those intracellular and extracellular factors that affect cell migrating velocity and cumulative number of trails in a biphasic or monotonic manner.

2. Materials and methods

2.1 Theoretical modeling

In this section we summarized the theoretical modeling with the simplified assumptions. Briefly [31,32], this model consists of three modules. The first two describe the signaling cascades responsible for cytoskeletal remodeling (Fig. 1a) and motor-clutch dynamics (Fig. 1b), respectively, which are governed by the coupled reaction-diffusion

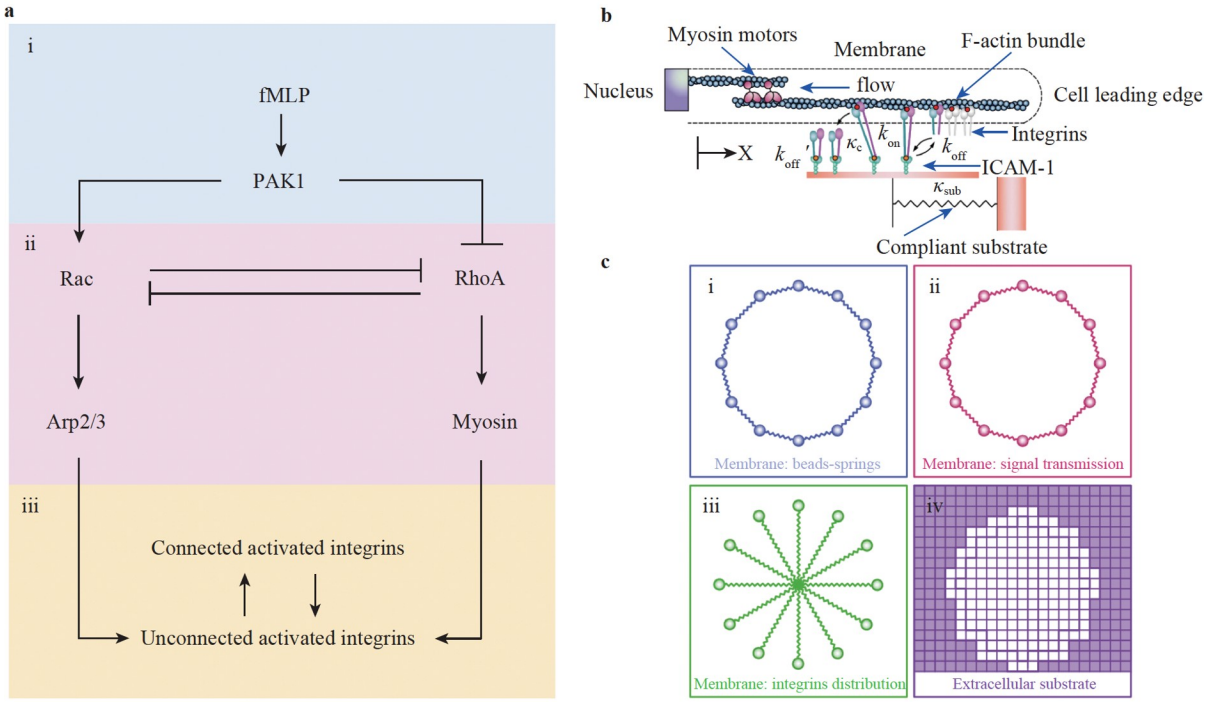

Figure 1 Theoretical modeling of chemotactic migration of a neutrophil on a compliant substrate, which is segregated into three modules: **a** module for signaling layers; **b** module for motor-clutch modeling; **c** module for cell mechanics.

equations. The third denotes cell mechanics and motility, which satisfies force-balance equations (Fig. 1c).

2.1.1 Module for signaling layers

This module involves three layers (Fig. 1a), i.e., (1) signal reception, (2) small Rho GTPase regulation, and (3) cytoskeletal effector regulation, as described previously [26]. Only newly-added in the module is the P21-activated kinase 1 (PAK1) pathway, which positively or negatively regulates Rac or RhoA signaling. For details of the mathematical descriptions, please refer to the Supplemental Materials and also Refs. [33,34].

2.1.2 Module for motor-clutch modeling

This module is applied to simulate the process of activated integrin bond break-up and cell trail formation on the substrate (Fig. 1b). On the ECM surface, the adhesive spots composed of integrins are uniformly distributed around the cell and subjected to the centripetal pulling by the F-actin microfilaments (Fig. 1c-iii). Integrins, serving as molecular clutches, reversibly engage the F-actin bundle to resist its retrograde flow. During mechanical loading, integrins may exist in four states: inactive and bound to the cytoskeleton (gray), activated and bound to the cytoskeleton (purple), bound to the ICAM-1 (green), or bound to both the ICAM-1 and the cytoskeleton (elongated purple). Myosin motors (pink) pull an F-actin (blue) filament bundle to the left with force. It is modified, from Ref. [19], by splitting those break-up sites of bound integrins into the two sets, the upper one binding to actin and the lower one binding to substrate. These molecular bonds tend to fail with a force-dependent off-rate at the lower (integrin-ICAM-1, orange) or upper (actin-integrin, red) binding sites and then form a neutrophil trail. The ECM deforms slightly via pulling integrins and receives those integrins left by the migrating cell when the trails are formed (Fig. 1c-iv). Here only the change in activated integrins is accounted in the module (Fig. 1b). For details of the formulations, please refer to the Supplemental Materials and also Ref. [16].

2.1.3 Module for cell mechanics

This module is used to simulate cell movement upon the chemotactic stimulation, as described previously [34]. The cell membrane is represented by discrete springs connected to multiple particle nodes (Fig. 1c-i) and the cell movement is governed by force balance equations [35]. Signal molecules located at each node are transmitted and interrelated with each other (Fig. 1c-ii). For detailed formulations, please refer to the Supplemental Materials and also Ref. [34].

2.2 Numerical simulations

Numerical calculations for both modules for signaling layers and cell mechanics were performed using self-developed algorithms and Matlab codes described previously [34]. Here only the calculations for the module for motor-clutch modeling were briefed, based on the algorithms in Ref. [16], as follows:

The key issue in these calculations is to define the fate of those active integrins bridging the ICAM-1 on substrate (lower break-up site) to the actin bundles (upper break-up site). Three criteria exist for determining the fate of integrins in the connected and unconnected states (n_l and n_u in Eq. S7 in the Supplemental Materials): (1) When the integrin is bound, $n_l^{t+1} = n_l^t + 1$, $n_u^{t+1} = n_u^t - 1$ after the current time step; (2) When the integrin is broken at the lower site, $n_l^{t+1} = n_l^t - 1$, $n_u^{t+1} = n_u^t + 1$ and the integrin is naturally disconnected; and (3) the integrin is broken at the upper site, $n_l^{t+1} = n_l^t - 1$, $n_u^{t+1} = n_u^t + 1$, $n_t^{t+1} = n_t^t + 1$ (n_t is the number of trails) and this broken integrin molecule at the original position is replaced by an activated integrin when it escapes from the cell (Fig. 1b). Note that the number of integrins here does not represent the actual number of integrin proteins in the experiments but just denote a qualitative consistency. Here the number of trails is defined as the number of integrin molecules that are ripped down from the cytoskeleton rather than broken up from the substrate. The trails so formed are then left on the substrate after the cell body moves forward, and visualized by fluorescence-labeled anti-β_2-integrin antibodies in the experiments, specified as below.

For each time step in the Monte Carlo simulation applied, molecular clutches are first allowed to associate with the F-actin bundle at a given on-rate, k_{on}. Next, the associated clutches are tested for the probability of dissociation based on their effective off-rate, k_{off} (Eq. S8 in the Supplemental Materials) and for the time duration required to break that clutch up, $t_i = -\ln(URN_i)/k_i$, for the ith binding or break-up event (URN_i is the random number and k_i the off-rate of the ith event). Once the last clutch is resolved, the final position of the substrate, x_{sub}, can be solved based on the force balance equation at the total force F and the systematic parallel spring constant K, as follows:

$$x_{sub} = \frac{F}{K} = \frac{\kappa_c \times \sum \Delta x}{n_l \times \kappa_c + \kappa_{sub}}, \tag{1}$$

where $\Delta x = v_f \cdot \Delta t$ defines the distance of an associated clutch at a time step Δt. From a given position of the substrate, the force against ongoing myosin motors is determined, and the velocity of F-actin retrograde flow, v_f, is calculated. Once the new retrograde velocity is determined, the associated clutch is displaced by a new distance $x + \Delta x$ and the force acting on each clutch is then re-calculated to determine the effective F-actin-clutch off-rate for the next time step.

All the parameters used in the simulations were summarized in Supplemental Tables S1-S3.

2.3 Experimental visualization of trail formation

Neutrophils stained with Alexa Fluor 488 anti-CD11a antibodies (Abcam, Cambridge, MA, USA) were added to the ICAM-1-immobilized surfaces with temperature control (37±0.5°C) and 5% CO_2 supply for live cell imaging. Time-lapsed immunofluorescence imaging was then captured at 30-s intervals for 15 min by confocal laser scanning microscopy (LSM880 NLO, Zeiss, Oberkochen, Germany) with a 63×/0.95NA objective. The velocity profiles of cellular protrusion and contraction were obtained by measuring the moving distance of cell frontmost and rearmost edges per 30-s, respectively, and the trail number was recorded synchronously. To monitor the time courses of neutrophil migration, time-lapsed differential interference contrast (DIC) imaging was captured separately at 30-s intervals for 15 min using an IX81 automatic inverted microscope (Olympus, Tokyo, Japan) equipped with an electron-multiplying charge-coupled device camera (iXon Ultra 897, Andor, UK). The tracks of migrating cells were identified with time using the manual tracking plugin interfaced with Image J. Various parameters including migrating velocity and distance were estimated off-line from cell centroid or frontmost and rearmost edges, using the Chemotaxis and Migration Tool 2.0 (IBIDI, Martinsried, Germany).

3. Results

3.1 Polarized distribution of cytoskeleton leads to directional migration of cells

First, polarized distributions of cell cytoskeleton were analyzed after fMLP stimulation. As exemplified in Fig. 2, those pericellular signaling molecules such as Rac and RhoA tend to be polarized and the distribution gradient is affected by the chemotactic gradient. Typically, PAK1 distribution starts to be polarized at t = 0 s and then its distribution gradient is positively correlated with the distance to the chemotactic source, decreasing from front to back (Fig. 2a). Here we assumed that the cell is subjected to a constant stimulus in the simulations for simplicity (Fig. 2b), even though the actual stimulus could be unstable experimentally. Thus, this stable polarized distribution of PAK1 in turn drives extracellular signaling molecules continue to modulate the polarized distribution of Rho GTPase along the plasma membrane, as seen in the differentially opposite distributions of activated Rac and RhoA along the cell circumference within 0-30 s (Fig. 2c). Both these Rho GTPase members yield bipolar distributions based on the antagonistic effects between them and the spatial regulation of PAK1. Specifically, the distribution of activated Rac presents a strong, stable gradient starting from the cell front, which is the same as the trend of upstream PAK1 signaling pathway (Fig. 2d). By contrast, RhoA also yields a stable polarized distribution at the cell rear, mainly based on the antagonistic effects of both Rac and PAK1 on the spatial

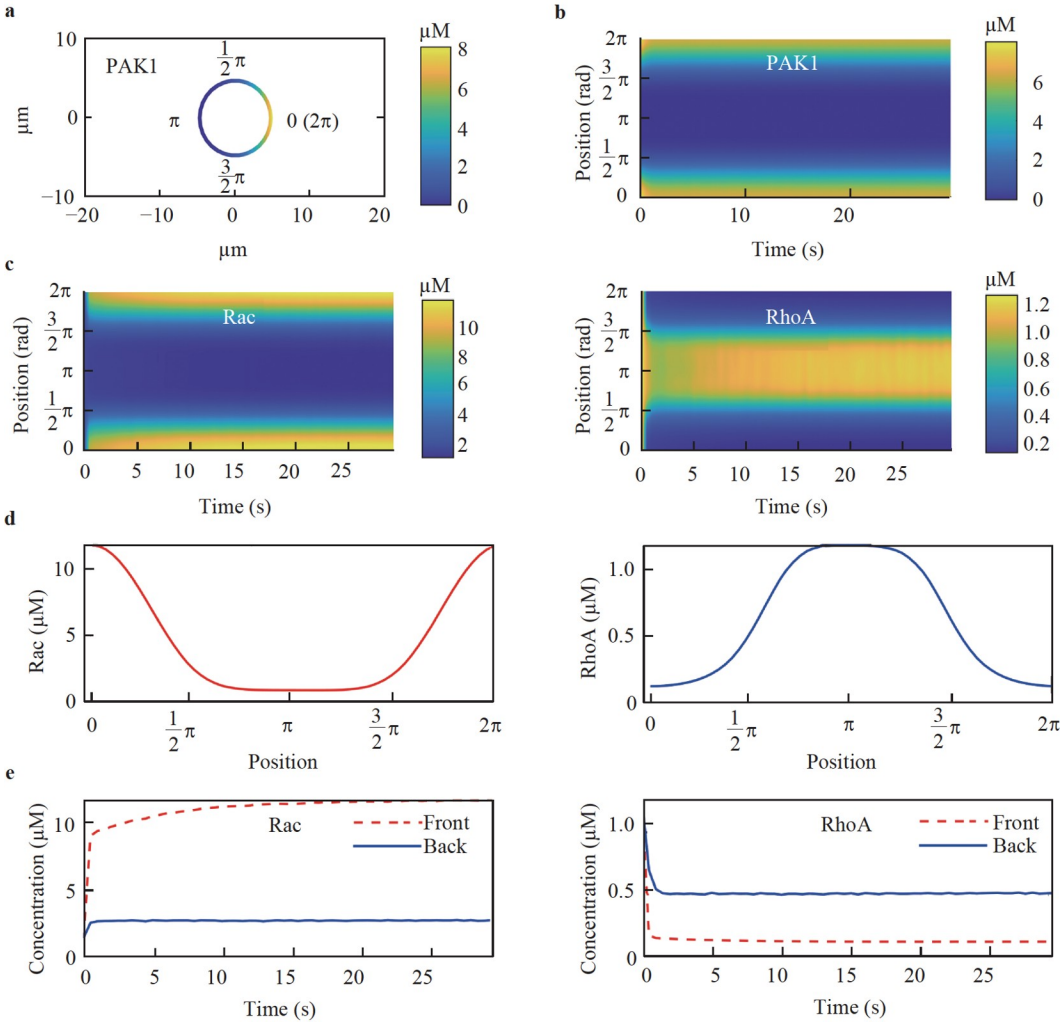

Figure 2 Polarized migration of a 10-μm diameter modeled neutrophil under fMLP gradient stimuli at a substrate hardness of 1 pN/nm. **a** PAK1 concentration along the cellular periphery. **b** Spatiotemporal evolution of PAK1. During t = 0-30 s, the cell receives the gradient chemotactic signals, leading to the polarized distribution of PAK1 molecules on the membrane. **c** Spatiotemporal evolutions of Rac (left) and RhoA (right). **d** Typical spatial distribution of Rac (left) and RhoA (right) concentrations at t = 30 s. **e** Time courses of Rac (left) and RhoA (right) concentrations.

modulation of RhoA (Fig. 2e).

These polarized Rac and RhoA molecules tend to regulate the cytoskeleton effectors Arp2/3 and myosin, resulting in Arp2/3 accumulation at the cell front and myosin concentration at the cell rear. An explicit boundary interface exists between Arp2/3 and myosin profiles at the cell rear (Fig. S1a-b), which is determined by mutually antagonistic effects between Rac and RhoA and also consistent with experimental observations in Ref. [36]. Concentrations of Arp2/3 and myosin manipulate the countercurrent velocity of intracellular microfilaments by adjusting the connections between integrin and substrate, which in turn regulates the forces acting on the cell, the migration dynamics and the trail number. The number of the unconnected integrins increases significantly at the cell rear after cell polarization and remains stable during cell migration. By contrast, the number of connected integrins is low initially along the pericellular membrane, and becomes high at the cell front after polarization (Fig. S1c-d). The reason for those sharp drop-offs of integrin number at 1/2π and 3/2π of the cell periphery is attributed to the imbalance between the rear polarization of myosin (seen in those visible interfaces in Fig. S1b) and the front polarization of connected integrin, based on the chemotactic gradient of PAK1 (Fig. 1b).

This low myosin concentration at the cell front enables those activated integrins to be polarized at the cell front when integrins bind to the substrate and start to accumulate (Fig. 3a). At the beginning of the fMLP simulation, various signaling molecules are assumed to be evenly distributed on the cell, and the molecular bonds between integrin and substrate are disconnected. Once it starts to migrate along fMLP gradient, the cell rapidly spreads outwards under the action of Arp2/3 and myosin. At this stage, the characteristic time of cell polarization is less than the one for binding integrins to the substrate, yielding almost no friction between the cell and the substrate and the rapidly increased

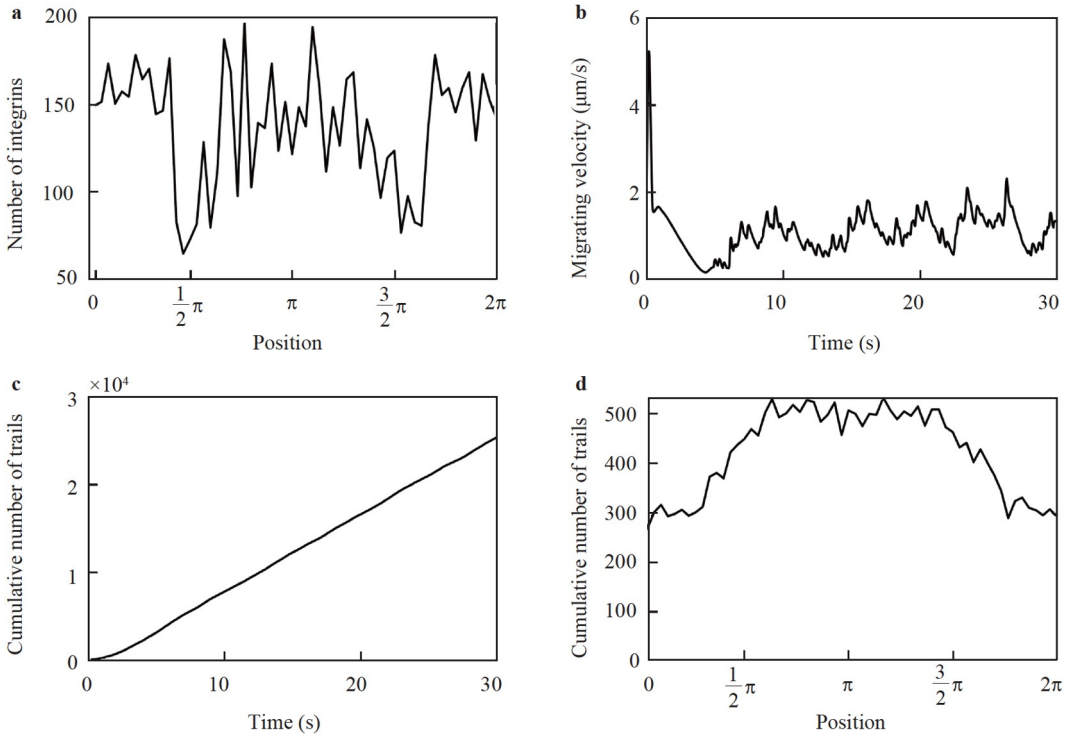

Figure 3 Spatiotemporal evolution of integrins and trails during chemotactic migration at a substrate hardness of 1 pN/nm. **a** Quantity distribution of activated integrins at t = 30 s. Activated integrins on the membrane appear to be polarized at the cell front and rear. **b** Variation of cell migrating velocity during t = 0-30 s. **c** Time course of the cumulative number of trails formed during t = 0-30 s. **d** Spatial distribution of the trails accumulated at cell periphery during t = 0-30 s.

cell area (Figs. 3b and S2a). Once the polarized distribution of molecules on the membrane is completed, Arp2/3 is concentrated at the cell front, which mainly produces forward traction, and integrins are attracted by myosin to be concentrated at the cell rear, which retracts the cell rear to generate backward traction and impedes cell movement by slowing down significantly the migrating velocity of the cell. In fact, integrin generates periodic connections under the action of myosin to provide periodic traction forces for cell migration while Arp2/3 generates stable protrusion, resulting in that the cell moves in the balance under the two active forces (Fig. S2b). During cell migration, differential distributions of myosins and integrins lead to distinct outcomes from the motor-clutch model. In terms of their quantities, increasing the myosin number causes integrins to break up more frequently while increasing the integrin number enables the duration for periodic rupture of integrin ensemble to be extended, resulting in a more stable traction force. The migrating velocity increases gradually, after a sharp fluctuation initially (< 3 s), and reaches to a plateau (Fig. 3b). Noting that the number of trails is defined as the number of integrin molecules that are ripped down from the upper site (attached to the cytoskeleton) rather than broken up from lower site (to the substrate), this number exhibits a transient increase with time and tends to maintain a constant trail formation rate after the migrating velocity reaches stable beyond t = 3 s (Fig. 3c). Trails are presented in all directions around the cell membrane, most of which is located at the cell rear (Fig. 3d).

3.2 Polarized integrin-substrate interactions dominates trail formation at the cell rear

Next, the trail formation of a migrating neutrophil was further elucidated based on the experimental observations and the theoretical modeling especially including the motor-clutch model. One experimental evidence lied in the polarized distribution of CD11a integrin and its co-localization with F-actin for a neutrophil having migrated over on an ICAM-1-immobilized substrate, presenting high CD11a expression at both the cell rear and front but high F-actin expression and partially-colocalized distribution with CD11a only at the cell front (Fig. 4a), where the distance at 0 μm denotes the cell frontmost. Meanwhile, our numerical simulations are in agreement with the above experimental observations. Calculated spatial distributions of integrins propose the similar pattern of the polarized integrins at the cell rear and front (Fig. 4b), confirming the availability of current numerical modeling. Here those molecules accumulated onto the membrane are projected vertically towards the center line of the cell (insert).

Another experimental evidence came from those differ-

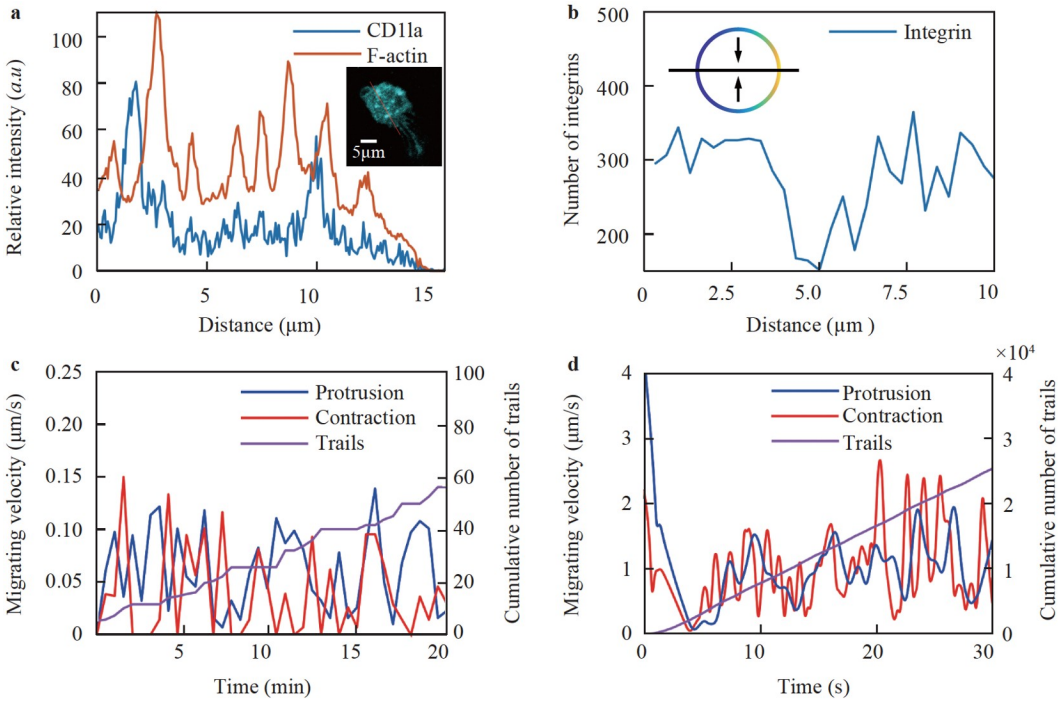

Figure 4 Comparisons between numerical simulations and experimental measurements of neutrophil migration. **a** Typical fluorescence intensity profiles (in *a.u.*) for CD11a (blue) and F-actin (orange) along the center line of a mouse neutrophil migrating on ICAM-1-immobilized substrate (red line in the insert). **b** Numerical simulations of integrin distributions along the radial direction of the cell (black line in the insert) at $t = 30$ s. **c** Typical trails number (purple) and protrusion (blue) or contraction (red) velocity profiles during a 20-min migration course. **d** Numerical simulations of protrusion (blue) or contraction (red) velocity and the number of trails formed (purple).

ential contraction and protrusion velocities of the migrating neutrophil. The protrusion or contraction velocity is defined as the moving distance of the cell frontmost or rearmost per min, respectively, and denoted as the polarized cell migration between cell front and rear edges. Both the contraction velocity at the cell rearmost and the protrusion velocity at the cell frontmost present similar fluctuating time courses even with slightly higher amplitudes for the former (left axis). The number of integrin patches left behind on the substrate is assumed to represent the number of trails formed, exhibiting almost a linear increase with time (right axis) (Fig. 4c). Again, numerical calculations supported the observations. Here the contraction and protrusion velocities both yield the fluctuating values, after initial drop, with similar time courses and slightly higher contraction amplitude. By contrast, the number of integrin patches increases with time monotonically (Fig. 4d). In fact, trail formation and cell migration are coupled together, including at least three interdependent events: cell front protrusion, rear contraction, and uropod detachment, in which polarized integrin-substrate interactions are critical in trail formation.

3.3 Extracellular factors regulates cell migration and trail formation

In order to determine which sets of model parameters are dominant in regulating cell migration and trail formation, all these parameters were segregated into two sets, i.e., extracellular and intracellular ones. The former includes substrate hardness, K_{sub}, and stimulation gradient of external chemoattractant, C, with five values each varying from 0.01-100 pN/nm and 0.1-5, respectively, as referred to those used in the motor clutch model [16]. Cell migration is determined by two forces along outward radial direction, i.e., one is affected by Arp2/3 and the other is related to integrin-substrate interactions. Forces generated at the cell front drive cell migration while those integrin and Arp2/3 accumulated at the cell rear play a role in spreading the cell and hindering the migration.

Time course of migrating velocity was first tested in terms of varied substrate hardness at a given chemotactic gradient of $C = 1$. The velocity exhibits a transition when it increases monotonically with time at an extremely low (0.01 pN/nm) or two high (10 and 100 pN/nm) hardness value(s), but fluctuates with time at two intermediate values (0.1 and 1 pN/nm) mainly due to periodic break-ups of integrin bonds (Fig. 5a). Plotting the mean velocity spanning over 0-30 s against substrate hardness yields a biphasic manner with the lowest value at 1 pN/nm (Fig. 5b), as expected [16], which attributes to the integrin-mediated robust adhesion and high traction forces on the substrate only at the appropriate hardness. By contrast, calculated spatial distributions

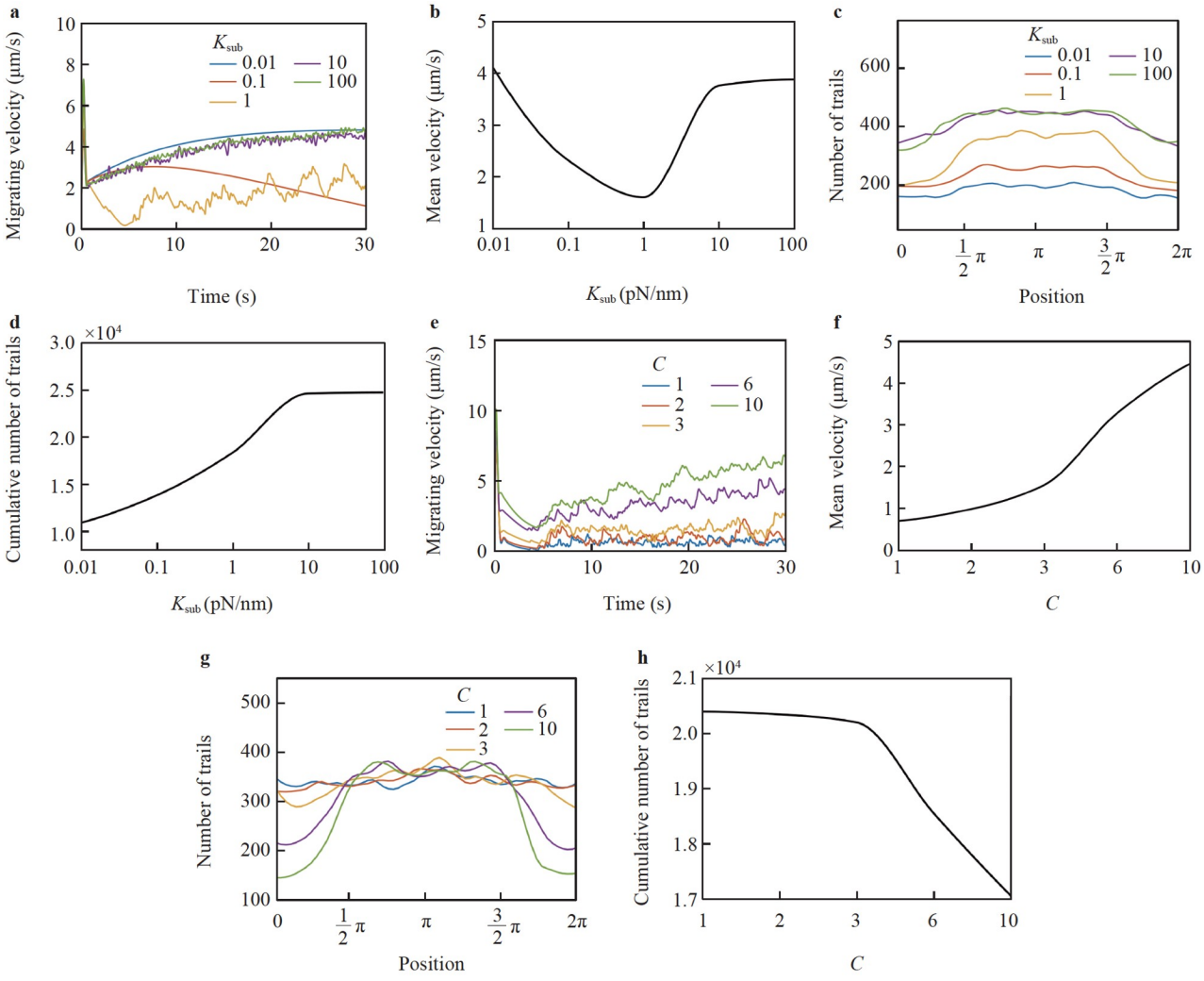

Figure 5 Parametric analyses of substrate hardness and chemical gradient on neutrophil migration. **a**, **b** Time courses of cell migrating velocity and mean velocity profile on substrate hardness at K_{sub} = 0.01-100 pN/nm. **c**, **d** Spatial distributions of trail number and cumulative trail number profile per cell on substrate hardness at K_{sub} = 0.01-100 pN/nm. **e**, **f** Time courses of cell migrating velocity and mean velocity profile on chemical gradient at C = 1-10. **g**, **h** Spatial distributions of trail number and cumulative trail number profile per cell on chemical gradient at C = 1-10.

imply the dominant occurrence of trails formed at cell rear at each given hardness (Fig. 5c). Again, summing all the trails formed over 0-30 s against substrate hardness presents a monotonic increase to reach a plateau threshold (Fig. 5d).

Time courses of migrating velocity were also tested in terms of the varied chemotactic gradient at a given substrate hardness of K_{sub} = 1 pN/nm. The velocity also exhibits a transition as it fluctuates and increases gradually with time at each gradient (Fig. 5e). Plotting the mean velocity spanning over 0-30 s against substrate hardness yields a monotonic increase (Fig. 5f). Again, calculated spatial distributions present the evenly distributed trails in cell periphery at the low gradient (0.1, 0.3 or 1) and the dominance of trail formation at cell rear at the high gradient (3 or 10) (Fig. 5g). Summing all the trails formed over 0-30 s against chemotactic gradient presents a stable phase initially followed by a sharp decrease with the increase of gradient (Fig. 5h).

3.4 Intracellular factors manipulate cell migration and trail formation

Multiple intracellular factors affect cell migration and trail formation. Here we mainly explored the effects of typical clutch on-rate, k_{on}, clutch unloaded off-rate, k_{off}, motor unloaded velocity, v_u, motor stall force, F_m, and number of clutches, n_c. Similar to those extracellular parametric dependences shown in Fig. 5, the time courses of migrating velocity present overall ascending trends with time (Fig. 6a, c, e, g, i) while the spatial distributions of trail numbers maintain the dominance of trails formed at cell rear (Fig. 6b, d, f, h, j) on varied values of each intracellular parameter. For simplicity, parametric analysis of mean velocity and cumulative number of trails was further conducted, as below.

The clutch on-rate k_{on} and unloaded off-rate k_{off} regulate

the forces exerted on the migrating cell via altering the association and dissociation duration of molecular bonds. Focusing on the off-rate at the lower site of the molecular bond, it was seen intuitively that mean velocity gradually increases and tends to reach a plateau (insert in Fig. 6a). This is because the average duration required to break up the molecular bonds decreases with the increase of unloaded off-rate, thus enhancing the migrating velocity after initial cell spreading. At the same time, the molecular bonds tend to break at the lower site, leading to the decreased cumulative number of trails with increase of the off-rate (insert in Fig. 6b). In contrast, the effect of the on-rate is opposite to the one of the off-rate. At the upper site that connects integrins to the cytoskeleton, similar ascending dependence of mean velocity but inverse ascending dependence of trails number are presented with increase of the off-rate at the

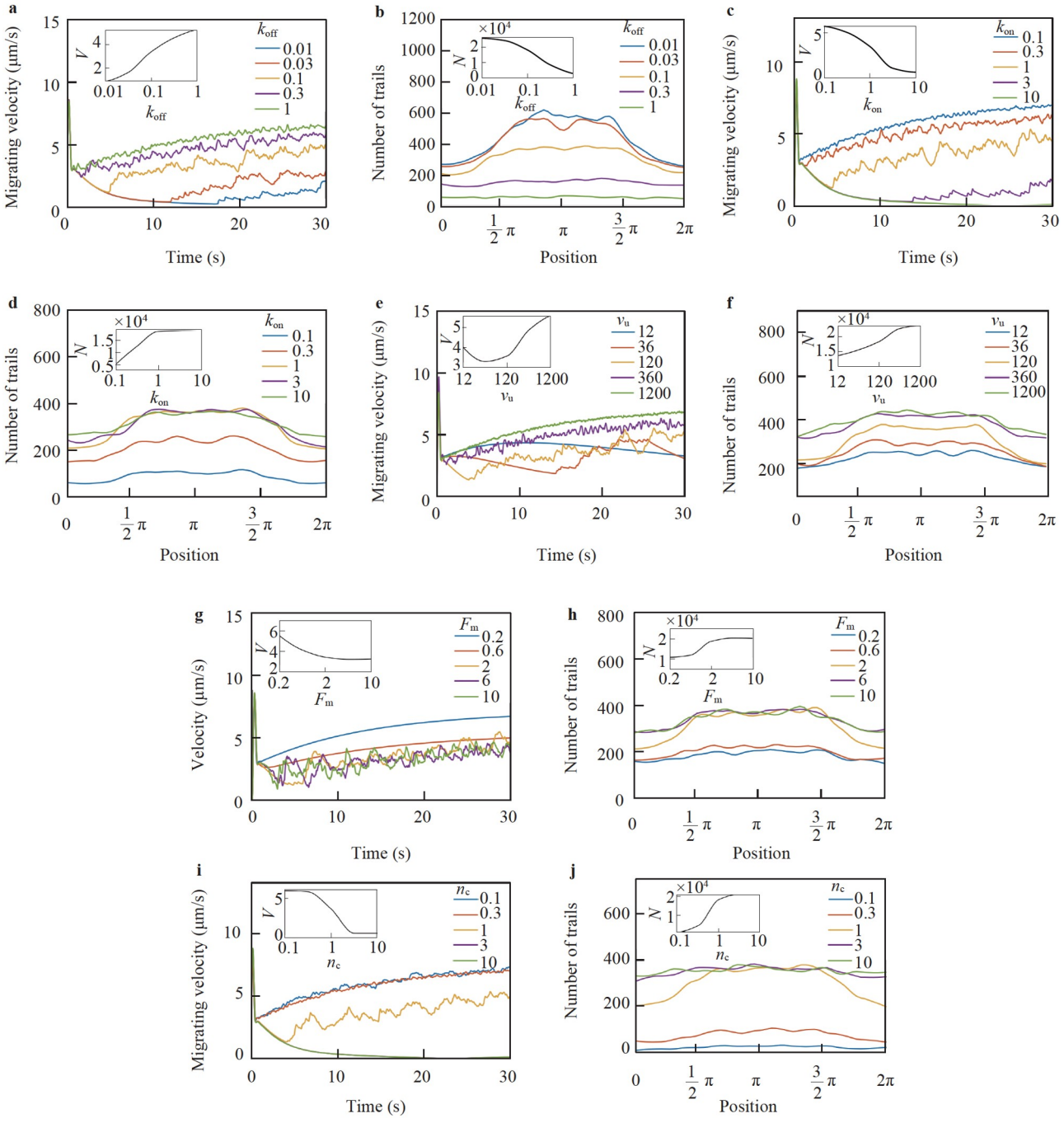

Figure 6 Parametric analyses of five motor-clutch parameters on neutrophil migration. Five values are selected for each parameter and spatiotemporal distributions of both migrating velocity and trail number are calculated, together with the profiles of mean velocity and cumulative trail number in each insert, as shown in Fig. 5. Here five parameters are tested including **a**, **b** clutch off-rate, **c**, **d** clutch on-rate, **e**, **f** motor unloaded velocity, **g**, **h** motor stall force, and **i**, **j** clutch number. Mean velocity V and cumulative number of trails N are abbreviated in the inserts for simplicity.

upper site k'_{off} (Fig. S3a-b), as compared to the above dependences for the unloaded off-rate at the lower site k_{off} (Fig. 6a-b). After completing the spreading, the cell with high on-rate rapidly interacts with the substrate and the mean velocity decreases rapidly (insert in Fig. 6c). This is presumably attributed to the polarized distribution of integrins at the cell rear, generating high traction forces to prevent the cell from moving forward. Meanwhile, the presence of myosin leads to the increase of trail number with increase of the on-rate to reach a plateau (insert in Fig. 6d), which is regulated by the motor contraction force limit that is relevant to the motor stall force F_m or the number of motors n_m.

The motor unloaded velocity v_u is influenced by the number of integrins in the bound state, since it governs the loading rate of integrin-motor bonds. A biphasic dependence of mean velocity is presented with the motor unloaded velocity (insert in Fig. 6e), similar to the effectiveness of substrate hardness. This is because the loading rate of the bonds is positively correlated by motor unloaded velocity, that is, slow loading is subjected to the low integrin-mediated traction while extremely fast loading causes collective failure of the integrin bonds, both of which promote fast cell migration. By contrast, the number of trails increases monotonically as the breakage of molecular bonds gradually increases mainly due to the increased unloading rate (insert in Fig. 6f).

The motor stall force F_m is mainly associated with the deceleration effect of retrograde flow of microfilaments after the integrins are connected to the substrate. The stronger the motor contraction the weaker the deceleration effect induced by those integrins connected to the microfilaments. This is determined by the intrinsic nature of the motor clutch model itself, and unlimited increase in F_m will not lead to further fast retrograde flow of F-actin in the model. Thus, increasing the motor contraction only promotes high forceful contraction of bound integrins, generating higher pulling forces and resulting in slower cell migration (insert in Fig. 6g). Meanwhile, the cumulative number of trails increases with F_m (insert in Fig. 6h). It is also noted that, when the motor stall force value is extremely high, the integrin-F-actin connection is almost impossible to slow down the retrograde flow velocity of the microfilaments and further increasing F_m will not affect both the migrating velocity and total trails number (Fig. 6g-h).

The rise in the number of clutches n_c only increases the number of integrins at the nodes, especially for those in the bound state. While integrins are still accumulated at the cell front and rear [37], the high concentration of myosin at the cell rear makes the integrins bear high pulling forces and enables the cell to migrate slowly (insert in Fig. 6i). By contrast, the cumulative number of trails exhibits a sigmoidal increase with increased number of integrins (insert in Fig. 6j). Trails so formed present two changes with varied number of integrins: one is that trails gradually increase with increase of integrin density and the other is that trails remain stable when the density is extremely high. In fact, the trails formed at an appropriate density tend to distribute more at the rear but less at the front, which is attenuated when the density is too high or too low.

4. Discussion

This work integrated a mechanochemical model with a motor-clutch model to predict the trail formation of a migrating neutrophil at the cell rear, which is crucial biologically for fast-phase cell migration. This type of cell migration is driven by rear contraction and front protrusion [34]. As illustrated in a working model proposed here (Fig. 7), the cell is subjected to both the protrusion force, F_p, of actin (dark or light cyan) polymerization inside the cell and the contraction force, F_r, of integrins pulling on the substrate (red arrows with varied thicknesses to indicate distinct magnitudes). After receiving extracellular chemotactic signals, the cell initiates immediately the polarized distributions of antagonistic Rac and RhoA via the balance-inhibition mechanisms, which then regulates the downstream effectors Arp2/3 and myosin and further the loca-

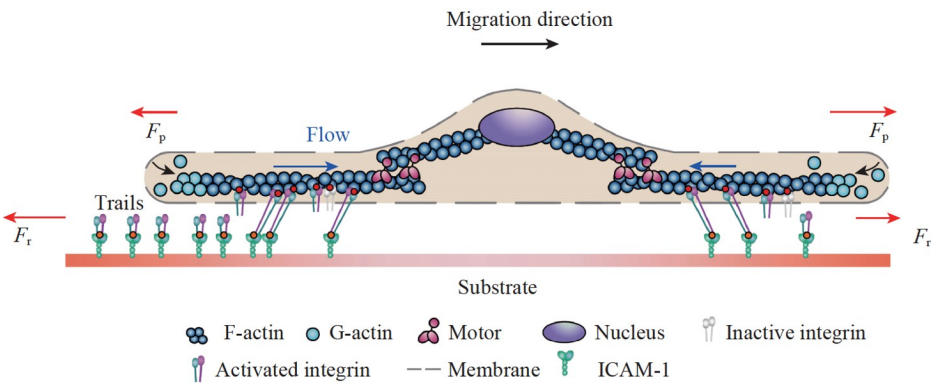

Figure 7 Working model of neutrophil trail formation on adherent substrate.

lized concentrations of integrins at the cell rear and front, finally manipulating the migrating velocity and the trail number. In this process, actin filaments tend to migrate towards the nucleus (purple) in response to motors (pink; blue arrows with varied thicknesses to indicate distinct magnitudes) and integrins may exist in four states, as indicated in Fig. 1b. The upper junctions (red) of most integrins are attached to the microfilaments and presented in an inactive form (gray), which can be activated by initiating the relevant signaling pathways. Once activated, the lower junctions (orange) of these integrins connect to their ICAM-1 ligands (green) on the substrate to generate traction forces. The integrin-ligand bonds are formed randomly at two binding sites, one connected to F-actin at the upper and another to the substrate at the lower. These bonds are stretched when F-actin filaments flow toward the cell center via myosin contraction and also generate traction forces via increased stress on the bonds, yielding two possible fates for the integrins that either break normally at the lower site to migrate away with cell body (open arrowheads) or at the upper site to be left on the substrate for trail formation (solid arrowheads). Thus, the cell presents two potential phenotypes of cell migration in either a trail-left or a persistent-moving way [38]. Cell migration is driven by rear contraction and front protrusion into a flat shape with central bulge. At cell front, less myosin exists and then the integrin can adhere stably. At cell rear, however, vast amount of myosin is accumulated, resulting in that those integrins at the rear are subjected to high traction forces and are readily broken than those at the front. Finally, trail remnants tend to be left mainly at the cell rear on the substrate once the integrin-actin bonds are broken up at the upper site (Fig. 7). Thus, this model allows to predict simultaneously the cell migrating velocity and the trail number with varied regulating parameters.

While numerous theoretical models exist for predicting the dynamics of cell migration on the substrate, it is still unclear how cell migration is associated with trail formation. At the cell level, our simulations indicated that the migrating velocity and trail number profiles can be illustrated by the spatiotemporal distributions of trails left along the pericellular direction or based on the corresponding cytoskeleton polarization. On one hand, several new aspects were added in this modeling. Compared with an existing model for one portion of cell migrating based on the interactions between integrins and the substrate [29], our model extends these interactions to the entire cell and achieves the same trend in the changes in molecular off-rates, which can be easily verified by experimental measurements. Meanwhile, the frictional flow between Arp2/3 and the substrate could contribute to the forward protrusion at cell front without cell retraction at the rear, described in a previous model [29]. In addition to those original motor-clutch models [16-19], an extra break-up site at the lower position was added into this model to simulate the generation of cell trails, together with applying those systematically-varied parameters in the original model. On the other hand, multiple assumptions were also adopted in this work. For example, integrin clustering proposed in the literature [39] is not presented in this model so that the force is directly transferred from the substrate to the cytoskeleton via integrins, which may lead to the overestimated number of trails due to the simplicity of treating the integrin-cytoskeleton linkage as a single bond rather than as a series of interactions. Another assumption in the model is that the traction force of integrins at the molecular level can affect cell migration but the cell migration feature is not directly represented in the connection of integrins to the cytoskeleton. Evidently, future tests on these newly-added aspects and assumptions on varied biological species or systems are meaningful to further extend the availability of this model.

Numerical predictions presented here are primarily consistent with those experimental observations from an *in vitro* neutrophil migration assay. Typically, F-actin presented a gradually declined distribution from the front to the rear while CD11a was concentrated at both the front and the rear (Figs. 4a-b), which could be interpreted by the regulation of signal pathways and the accumulation of local integrins. For example, blebbistatin treatment inhibits intracellular myosin activity, equating to the decrease in F_m in the model, and thus the enhanced migrating velocity of these treated cells is likely caused by the reduced traction forces of integrins at the rear, after myosin inhibition [40]. Cells are attached onto the substrate through integrins and the substrate hardness in turn affects the loading rate of integrin bonds, resulting in the small traction on slow loading or the rapid disconnection on fast loading [3]. In fact, the rear contraction and the front protrusion velocities were not synchronous and the fluctuating amplitude for the former was higher than that the latter, which was evidently related to the size and stability of traction forces provided by integrins (Figs. 4c-d). At the front, the forces generated by Arp2/3 and integrin both point forward and provide stable driving forces for cell migration. The forces produced by Arp2/3 and integrin at the rear, however, both point backward with the difference that the one produced by Arp2/3 is stable while the other generated by integrin serves as the waved forces due to its periodic binding and break-up. Thus, the reasoning that the cell moves forward but not backward is due to the polarization of Arp2/3 to exert high forces at the front. Consequently, the number of trails (integrins) increases monotonically with time (Figs. 4c-d).

Numerous parameters in the model affect the migrating velocity and the trail number. No matter whether they are extracellular or intracellular, their regulating effects on cell migration can be divided into biphasic or monotonic de-

pendence as well as positively or negatively monotonic dependence. For example, either substrate hardness or motor unloaded velocity can regulate the migrating velocity in a biphasic pattern (Figs. 5b and 6e), that is, an optimized value exists at which the traction force derived from integrins can be maximally transferred to the substrate. As a factor that is significantly altered after organ lesions, substrate hardness plays an important role in cell migration in living organisms [41,42]. At low or high hardness, the cell migration is likely governed by Arp2/3. At moderate hardness, integrins can provide sufficient traction force, due to their polarized distribution at the cell rear, to slow down the cell migration. Since the traction force provided by integrins reaches its maximum at this time, the migrating velocity oscillates with the periodicity of integrin bond break-up (Figs. 5a-b). Notably, these integrins in this model have two potential break-up sites. While these two sites present the same effect on cell migration to promote cell migration, their effects on trail formation is completely opposite, with a favorable upper site but a disadvantageous lower site. An increase in the off-rate at the upper site leads to an increase in the number of trails so formed (Fig. S3). It is also noticed that the external chemotactic gradient can shorten the duration of cytoskeleton polarization, then promoting cell migration and lowering trail formation with increased gradient (Fig. 5f-h). In fact, an increase in integrin density leads to an increase in the number of trails. At this point, high fractions of integrins tend to break spontaneously before being pulled, leading to the increase of trails appearing along the cell periphery without polarization (Fig. 6j). Evidently, further parametric analysis is required to quantify their impacts by either altering these parameter values or extending those potential parameters that have not been included in this work. It is also noted that membrane tension affects cell migration through regulating the protrusion and the stiffness of actin filaments varies with the increase of actin length, thus affecting the activities of cortical cytoskeleton [43,44], which will tested in the future modeling.

In conclusion, the profiles of migrating velocity and trail formation of a migrating cell were investigated by developing a cell migration model and the effects of multiple regulating factors were tested systematically. Force-balance mechanisms were depicted for trail formation at the molecular and cellular levels and the resulted simulations were in agreement with experimental observations. This model is expected to elucidate how both physical and chemical interactions work cooperatively to affect the complicated process of fast cell migration and specific trail formation.

Author contributions *Xiaoning Zhang, Yan Zhang, and Mian Long developed the concept, designed the simulations, analyzed the data, wrote the paper, revised and edited the final version. Xiaoning Zhang developed mathematical model and conducted numerical simulations. Wenhui Hu and Wenbo Gao performed experiments.*

Acknowledgements *This work was supported by the National Natural Science Foundation of China (Grant Nos. 31627804, 11772345, and 91539119), the Scientific Instrument Developing Project of the Chinese Academy of Sciences (Grant No. GJJSTU20220002), and Frontier Science Key Project of Chinese Science Academy (Grant No. QYZDJ-SSW-JSC018).*

1 C. Summers, S. M. Rankin, A. M. Condliffe, N. Singh, A. M. Peters, and E. R. Chilvers, Neutrophil kinetics in health and disease, Trends Immunol. **31**, 318 (2010).
2 A. Mantovani, M. A. Cassatella, C. Costantini, and S. Jaillon, Neutrophils in the activation and regulation of innate and adaptive immunity, Nat. Rev. Immunol. **11**, 519 (2011).
3 C. Nathan, Neutrophils and immunity: Challenges and opportunities, Nat. Rev. Immunol. **6**, 173 (2006).
4 E. M. Gardiner, K. N. Pestonjamasp, B. P. Bohl, C. Chamberlain, K. M. Hahn, and G. M. Bokoch, Spatial and temporal analysis of Rac activation during live neutrophil chemotaxis, Curr. Biol. **12**, 2029 (2002).
5 C. A. Parent, Making all the right moves: Chemotaxis in neutrophils and Dictyostelium, Curr. Opin. Cell Biol. **16**, 4 (2004).
6 K. Lim, Y. M. Hyun, K. Lambert-Emo, T. Capece, S. Bae, R. Miller, D. J. Topham, and M. Kim, Neutrophil trails guide influenza-specific $CD8^+$ T cells in the airways, Science **349**, 11 (2015).
7 J. A. Broussard, D. J. Webb, and I. Kaverina, Asymmetric focal adhesion disassembly in motile cells, Curr. Opin. Cell Biol. **20**, 85 (2008).
8 B. H. Ji, and B. Huo, Probing the mechanosensitivity in cell adhesion and migration: Experiments and modeling, Acta Mech. Sin. **29**, 469 (2013).
9 S. L. Gupton, and C. M. Waterman-Storer, Spatiotemporal feedback between actomyosin and focal-adhesion systems optimizes rapid cell migration, Cell **125**, 1361 (2006).
10 L. B. Case, and C. M. Waterman, Integration of actin dynamics and cell adhesion by a three-dimensional, mechanosensitive molecular clutch, Nat. Cell. Biol. **17**, 955 (2015).
11 G. Salbreux, G. Charras, and E. Paluch, Actin cortex mechanics and cellular morphogenesis, Trends Cell Biol. **22**, 536 (2012).
12 D. L. Bodor, W. Pönisch, R. G. Endres, and E. K. Paluch, Of cell shapes and motion: The physical basis of animal cell migration, Dev. Cell **52**, 550 (2020).
13 N. Li, D. Mao, S. Lü, C. Tong, Y. Zhang, and M. Long, Distinct binding affinities of Mac-1 and LFA-1 in neutrophil activation, J. Immunol. **190**, 4371 (2013).
14 S. He, X. Li, and B. Ji, Mechanical force drives the polarization and orientation of cells, Acta Mech. Sin. **35**, 275 (2019).
15 R. O. Hynes, Integrins: Versatility, modulation, and signaling in cell adhesion, Cell **69**, 11 (1992).
16 B. L. Bangasser, S. S. Rosenfeld, and D. J. Odde, Determinants of maximal force transmission in a motor-clutch model of cell traction in a compliant microenvironment, Biophys. J. **105**, 581 (2013).
17 N. Li, S. Lü, Y. Zhang, and M. Long, Mechanokinetics of receptor–ligand interactions in cell adhesion, Acta Mech. Sin. **31**, 248 (2015).
18 J. Wei, X. Chen, and B. Chen, Harnessing structural instability for cell durotaxis, Acta Mech. Sin. **35**, 355 (2019).
19 C. E. Chan, and D. J. Odde, Traction dynamics of filopodia on compliant substrates, Science **322**, 1687 (2008).
20 C. G. Gahmberg, Leukocyte adhesion: CD11/CD18 integrins and intercellular adhesion molecules, Curr. Opin. Cell Biol. **9**, 643 (1997).
21 K. Ley, C. Laudanna, M. I. Cybulsky, and S. Nourshargh, Getting to the site of inflammation: The leukocyte adhesion cascade updated, Nat. Rev. Immunol. **7**, 678 (2007).
22 T. Yago, B. Shao, J. J. Miner, L. Yao, A. G. Klopocki, K. Maeda, K. M. Coggeshall, and R. P. McEver, E-selectin engages PSGL-1 and CD44 through a common signaling pathway to induce integrin $\alpha_L\beta_2$-mediated slow leukocyte rolling, Blood **116**, 485 (2010).
23 S. Nourshargh, and R. Alon, Leukocyte migration into inflamed tissues, Immunity **41**, 694 (2014).

24 Y. Gong, Y. Zhang, S. Feng, X. Liu, S. Lü, and M. Long, Dynamic contributions of P- and E-selectins to β_2-integrin-induced neutrophil transmigration, FASEB J. **31**, 212 (2017).
25 T. Lämmermann, and M. Sixt, Mechanical modes of 'amoeboid' cell migration, Curr. Opin. Cell Biol. **21**, 636 (2009).
26 S. Feng, L. Zhou, Y. Zhang, S. Lü, and M. Long, Mechanochemical modeling of neutrophil migration based on four signaling layers, integrin dynamics, and substrate stiffness, Biomech. Model. Mechanobiol. **17**, 1611 (2018).
27 E. Ghabache, Y. Cao, Y. Miao, A. Groisman, P. N. Devreotes, and W. Rappel, Coupling traction force patterns and actomyosin wave dynamics reveals mechanics of cell motion, Mol. Syst. Biol. **17**, 21 (2021).
28 S. P. Palecek, A. F. Horwitz, and D. A. Lauffenburger, Kinetic model for integrin-mediated adhesion release during cell migration, Ann. Biomed. Eng. **27**, 219 (1999).
29 A. Macdonald, A. R. Horwitz, and D. A. Lauffenburger, Kinetic model for lamellipodal actin-integrin 'clutch' dynamics, Cell Adhes. Migration **2**, 95 (2008).
30 R. Oria, T. Wiegand, J. Escribano, A. Elosegui-Artola, J. J. Uriarte, C. Moreno-Pulido, I. Platzman, P. Delcanale, L. Albertazzi, D. Navajas, X. Trepat, J. M. García-Aznar, E. A. Cavalcanti-Adam, and P. Roca-Cusachs, Force loading explains spatial sensing of ligands by cells, Nature **552**, 219 (2017).
31 A. F. M. Marée, A. Jilkine, A. Dawes, V. A. Grieneisen, and L. Edelstein-Keshet, Polarization and movement of keratocytes: A multiscale modelling approach, Bull. Math. Biol. **68**, 1169 (2006).
32 J. Xu, X. L. Wang, Y. Q. Liu, and X. B. Gong, A cellular scale numerical study of the effect of mechanical properties of erythrocytes on the near-wall motion of platelets, Acta Mech. Sin. **30**, 274 (2014).
33 S. L. Feng, L. W. Zhou, S. Q. Lü, and Y. Zhang, Dynamic seesaw model for rapid signaling responses in eukaryotic chemotaxis, Phys. Biol. **15**, 056004 (2018).
34 L. Zhou, S. Feng, L. Li, S. Lü, Y. Zhang, and M. Long, Two complementary signaling pathways depict eukaryotic chemotaxis: A mechanochemical coupling model, Front. Cell Dev. Biol. **9**, 12 (2021).
35 S. Chen, J. Zhu, J. Xue, X. Wang, P. Jing, L. Zhou, Y. Cui, T. Wang, X. Gong, S. Lü, and M. Long, Numerical simulation of flow characteristics in a permeable liver sinusoid with leukocytes, Biophys. J. **121**, 4666 (2022).
36 L. Gambardella, and S. Vermeren, Molecular players in neutrophil chemotaxis—focus on PI3K and small GTPases, J. Leukocyte Biol. **94**, 603 (2013).
37 V. Andasari, D. Lü, M. Swat, S. Feng, F. Spill, L. Chen, X. Luo, M. Zaman, and M. Long, Computational model of wound healing: EGF secreted by fibroblasts promotes delayed re-epithelialization of epithelial keratinocytes, Integr. Biol. **10**, 605 (2018).
38 J. Lin, Y. Wang, and J. Qian, Effects of domain unfolding and catch-like dissociation on the collective behavior of integrin-fibronectin bond clusters, Acta Mech. Sin. **37**, 229 (2021).
39 Y. Zhong, and B. Ji, Impact of cell shape on cell migration behavior on elastic substrate, Biofabrication **5**, 015011 (2013).
40 Z. Liu, L. A. van Grunsven, E. Van Rossen, B. Schroyen, J. P. Timmermans, A. Geerts, and H. Reynaert, Blebbistatin inhibits contraction and accelerates migration in mouse hepatic stellate cells, Br. J. Pharmacol. **159**, 304 (2010).
41 R. Sridharan, B. Cavanagh, A. R. Cameron, D. J. Kelly, and F. J. O'Brien, Material stiffness influences the polarization state, function and migration mode of macrophages, Acta Biomater. **89**, 47 (2019).
42 R. Sridharan, D. J. Kelly, and F. J. O'Brien, Substrate stiffness modulates the crosstalk between mesenchymal stem cells and macrophages, J. Biomech. Eng. **143**, 031001 (2021).
43 K. Tao, J. Wang, X. Kuang, W. Wang, F. Liu, and L. Zhang, Tuning cell motility via cell tension with a mechanochemical cell migration model, Biophys. J. **118**, 2894 (2020).
44 S. H. Li, H. Gao, and G. K. Xu, Network dynamics of the nonlinear power-law relaxation of cell cortex, Biophys. J. **121**, 4091 (2022).

中性粒细胞在基底上迁移过程中曳尾形成的理论模型

张晓宁, 胡文慧, 高文博, 章燕, 龙勉

摘要 中性粒细胞通过头部前伸和尾部收缩可以在内皮细胞或细胞外基质上快速迁移. 这些细胞在迁移的过程中会遗留下大量富含整合素的膜结构, 但目前尚不清楚曳尾的形成与细胞迁移之间的定量关系以及在这一过程中起关键作用的调控因素. 本文将多层级力学-化学耦合模型与细胞迁移的马达-离合器模型相结合, 对中性粒细胞在基质上的趋化迁移进行了数值模拟. 结果表明, 随着PAK1和其下游信号分子Rac和RhoA的极化分布, 细胞膜上的整合素倾向于在细胞前后两端产生极化积聚, 当Arp2/3和myosin分别在细胞的头尾极化时, 细胞会在整合素的作用下增大迁移速度并提高曳尾的数量. 这些关于整合素极化以及曳尾形成的预测与典型的实验结果一致. 参数分析进一步表明, 虽然细胞迁移速度与基底硬度和"马达"空载速度呈现双相依赖关系, 但是曳尾形成的数量随着基底硬度、整合素-配体分子键的结合率、"马达"空载速度、"马达"空载拉力和"离合器"数量的增加而单调增加, 随着趋化因子浓度和整合素-配体分子键的解离率的增加而减少. 上述工作为阐明中性粒细胞迁移的力学-化学-生物学耦合过程和探究调节中性粒细胞迁移过程中影响曳尾形成的关键因素提供了一种解释.